

Effects of Temperature and Pressure on the Magnetic Properties of $\text{La}_{1-x}\text{Pr}_x\text{CoO}_3$

Anatoliy S. Panfilov, Anastasiya A. Lyogenkaya,* Gennadiy E. Grechnev, Volodymyr A. Pashchenko, Leonid O. Vasylechko, Vasyl M. Hreb, and Andrei V. Kovalevsky

For $\text{La}_{1-x}\text{Pr}_x\text{CoO}_3$ cobaltites with $x = 0, 0.1, 0.2,$ and $0.3,$ the temperature dependence of magnetic susceptibility $\chi(T)$ is studied in the temperature range from 5 to 400 K. Also, the crystal structure of these cobaltites is investigated, and the effect of hydrostatic pressure up to 2 kbar on their susceptibility is measured at fixed temperatures $T = 78, 150,$ and 300 K. The specific dependencies $\chi(T)$ and the large negative pressure effect observed in $\text{La}_{1-x}\text{Pr}_x\text{CoO}_3$ are assumed to arise from Co^{3+} ions, which contribution to the total susceptibility is evaluated using $\text{La}_{1-x}\text{Pr}_x\text{AlO}_3$ as a reference system. The obtained experimental data on temperature and pressure effects in magnetism are analyzed in the framework of a two-level model with energy gap Δ between the ground state of the system with zero spin of Co^{3+} ions and the excited higher-spin state. In this model, magnetism of Co^{3+} ions is determined by the temperature-induced population of the excited state, and the magnitude of the pressure effect is governed by the volume dependence of Δ . The results of the analysis, supplemented by the theoretical calculations of the electronic structures of LaCoO_3 and $\text{PrCoO}_3,$ indicate a significant increase in Δ with a decrease in the unit cell volume both under hydrostatic pressure and by substituting La with Pr having a smaller ionic radius. The estimated effects of the physical and chemical pressures on Δ and χ are similar in magnitude, indicating a strong correlation of the spin state of Co^{3+} ions with the lattice volume.

1. Introduction

In RCO_3 cobaltites, which have perovskite-like crystal structures, the Co^{3+} ions can exist in three different spin states, corresponding to the low (LS, $S = 0$), intermediate (IS, $S = 1$) and high (HS, $S = 2$) spin values. The energy difference between these states, determined by the competition between the splitting of the ionic energy levels by the crystal field in t_{2g} and e_g states and Hund's intra-atomic exchange interaction, is rather small. As a result, the relative positions of these spin states appear to be very sensitive to external factors such as temperature, pressure, and magnetic field. This situation generates different spin crossovers and provides the observed peculiar behavior and variety of physical properties of the RCO_3 systems (see the studies by Raveau and Seikh and Takami^[1–3] and references therein).

The large number of investigations of physical properties of RCO_3 cobaltites were conducted to reveal the scenario of transition between spin states of Co^{3+} ions with increasing temperature. In a number of experimental and theoretical papers,^[4–10] the authors proposed the LS \rightarrow HS-type

scenario to explain the physical properties of RCO_3 . In contrast, many works have given evidence in favor of the LS \rightarrow IS scenario.^[11–17] Therefore, the nature of different spin states of Co^{3+} ions in RCO_3 and their transformation under external and chemical pressures are still the subjects of active experimental and theoretical studies.

The transitions between the spin states of Co^{3+} with increasing temperature is most clearly manifested in the magnetic properties of LaCoO_3 compound, where La has no magnetic moment and the contribution of cobalt ions to the total susceptibility χ appears to be predominant. At low temperatures, LaCoO_3 is in the ground LS state ($S = 0$), being a nonmagnetic semiconductor. With increasing temperature, the states of a higher spin, IS and/or HS, begin to be populated, leading to a rapid increase in magnetic susceptibility and a pronounced maximum in $\chi(T)$ at $T \approx 100$ K, followed by a decrease in susceptibility close to the Curie–Weiss law.^[13,14,18] Results of a detailed analysis of the temperature dependence of magnetic susceptibility in

Dr. A. S. Panfilov, Dr. A. A. Lyogenkaya, Prof. G. E. Grechnev, Dr. V. A. Pashchenko
B. Verkin Institute for Low Temperature Physics and Engineering
National Academy of Sciences of Ukraine
61101 Kharkov, Ukraine
E-mail: lyogenkaya@ilt.kharkov.ua

Prof. L. O. Vasylechko, V. M. Hreb
Lviv Polytechnic National University
79013 Lviv, Ukraine

Prof. A. V. Kovalevsky
Department of Materials and Ceramic Engineering
CICECO – Aveiro Institute of Materials
University of Aveiro
3810-193 Aveiro, Portugal

The ORCID identification number(s) for the author(s) of this article can be found under <https://doi.org/10.1002/pssb.202000085>.

DOI: 10.1002/pssb.202000085

1 LaCoO_3 ^[13,14] convincingly argue in favor of the LS→IS scenario
2 of the spin crossover, which is valid at least for the range of low
3 and moderate temperatures. In addition, an important result of
4 this analysis is the evaluated temperature dependence of the
5 energy difference between IS and LS states, which decreases
6 with increase in temperature and vanishes at about room
7 temperature.

8 One of the efficient ways to further investigate the phenom-
9 non of spin crossover is to study the effect of high pressure on
10 the magnetic properties of cobaltites. Such investigations for
11 LaCoO_3 ^[19-22] and for a number of RCoO_3 compounds ($\text{R} = \text{Pr}$,
12 Nd , Sm , and Eu)^[21] have revealed a strong decrease under
13 pressure of the Co ions' contribution to the total susceptibility
14 and a shift of the characteristic maximum on $\chi(T)$ dependence
15 to higher temperatures.

16 A number of investigations were based on the studies of the
17 Co^{3+} spin state in $\text{La}_{1-x}\text{R}_x\text{CoO}_3$ compounds. In these com-
18 pounds, the substitution of La with rare-earth elements has pro-
19 vided a decrease in the cell volume due to a decrease in the ionic
20 radius along the R^{3+} series. The corresponding effects of chemi-
21 cal pressure on magnetic susceptibility of $\text{La}_{1-x}\text{Pr}_x\text{CoO}_3$,^[23]
22 $\text{La}_{1-x}\text{Nd}_x\text{CoO}_3$,^[24] $\text{La}_{1-x}\text{Sm}_x\text{CoO}_3$,^[25] and $\text{La}_{1-x}\text{Eu}_x\text{CoO}_3$ ^[14,26]
23 revealed some similarity in the behavior of magnetism of
24 Co^{3+} ions in these compounds with the relevant effects of
25 physical pressure in LaCoO_3 . However, it should be noted that
26 a quantitative analysis of the spin state of Co^{3+} ions in such
27 systems, based on their magnetic properties, requires proper
28 account of the rare-earth background magnetism.

29 In this article, we provide the results of extensive studies of
30 structural and magnetic properties of $\text{La}_{1-x}\text{Pr}_x\text{CoO}_3$ com-
31 pounds. The main goal of this work is to explore the dependence
32 of the spin state of cobalt ions in these compounds on tempera-
33 ture, as well as on the lattice volume changes, both under hydro-
34 static pressure and by substituting La with Pr, which has a
35 smaller ionic radius. For this purpose, we have investigated
36 the magnetic susceptibility of the isostructural $\text{La}_{1-x}\text{Pr}_x\text{CoO}_3$
37 cobaltites ($0 \leq x \leq 0.3$) in the temperature range 5–400 K,
38 and also under applied hydrostatic pressure up to 2 kbar at fixed
39 temperatures $T = 78$, 150, and 300 K. The experimental data on
40 the excitation energies Δ and their pressure derivatives were ana-
41 lyzed using the corresponding theoretical estimates for LaCoO_3
42 and PrCoO_3 obtained by the ab initio calculations based on the
43 fixed spin moment method.^[27]

44 2. Experimental Section

45 2.1. Preparing and Crystal Structure Study of $\text{La}_{1-x}\text{Pr}_x\text{CoO}_3$ 46 Compounds

47 The powder samples of $\text{La}_{1-x}\text{Pr}_x\text{CoO}_3$ ($x = 0, 0.1, 0.2$ and 0.3)
48 were prepared by conventional solid-state method using
49 high-purity La_2O_3 (Sigma Aldrich, $\geq 99.9\%$), Pr_6O_{11} (Sigma
50 Aldrich, 99.9%), and Co_3O_4 (Sigma Aldrich, 99.5%). Before
51 weighing, lanthanum oxide was calcined at 973 K for 2 h in
52 air to remove moisture. Praseodymium oxide was annealed at
53 1273 K for 2 h with 3°C min^{-1} cooling and heating rates to
54 remove absorbed species and attain the equilibrium composition
55 of Pr_6O_{11} , confirmed by XRD. The precursor powders were

mixed in stoichiometric proportion and calcined consecutively 1
at 1173, 1273, and 1323 K for 10 h at each temperature, with inter- 2
mediate regrindings. Resulting powders were uniaxially compacted 3
as disk-shaped samples and sintered at 1373 K for 24 h. 4

Phase and structural characterizations of the samples were 5
carried out using Rigaku D/Max-B and modernized DRON-3M 6
powder diffractometers (Cu $\text{K}\alpha$ radiation, $\lambda = 1.54185 \text{ \AA}$). Crystal 7
structure parameters including unit cell dimensions, coordinate, 8
and isotropic displacement parameters of atoms were derived 9
from the diffraction data collected in 2θ range of 20° – 125° by 10
full profile Rietveld refinement applying WinCSD program 11
package.^[28] 12

Examination of XRD patterns of the $\text{La}_{1-x}\text{Pr}_x\text{CoO}_3$ materials 13
had revealed pure rhombohedral perovskite structure for the 14
samples with $x = 0.1$ and 0.2 (Figure 1). The main features of 15
XRD pattern of $\text{La}_{0.7}\text{Pr}_{0.3}\text{CoO}_3$ material were similar to the afore- 16
mentioned specimens. Nevertheless, the careful examination of 17
the pattern allowed to detect extra features, which cannot be 18
described in a single $R\bar{3}c$ structural model (Figure 1). This obser- 19
vation pointed to the coexistence of rhombohedral and ortho- 20
rhombic perovskites in the sample with nominal composition 21
 $\text{La}_{0.7}\text{Pr}_{0.3}\text{CoO}_3$. This coexistence was in excellent agreement with 22
the data of thorough X-ray synchrotron powder diffraction investi- 23
gation of RCoO_3 - $\text{R}'\text{CoO}_3$ ($\text{R}, \text{R}' = \text{La}, \text{Pr}, \text{Nd}, \text{Sm}$) systems,^[29] 24
according to which the phase-separation region occurred in 25
 $\text{La}_{1-x}\text{Pr}_x\text{CoO}_3$ perovskite materials at $0.25 \leq x \leq 0.4$. 26

Phase composition and crystal structure of the materials stud- 27
ied were fully confirmed by full-profile Rietveld refinement. 28
For the $\text{La}_{1-x}\text{Pr}_x\text{CoO}_3$ samples with $x = 0.1$ and 0.2 , an excellent 29

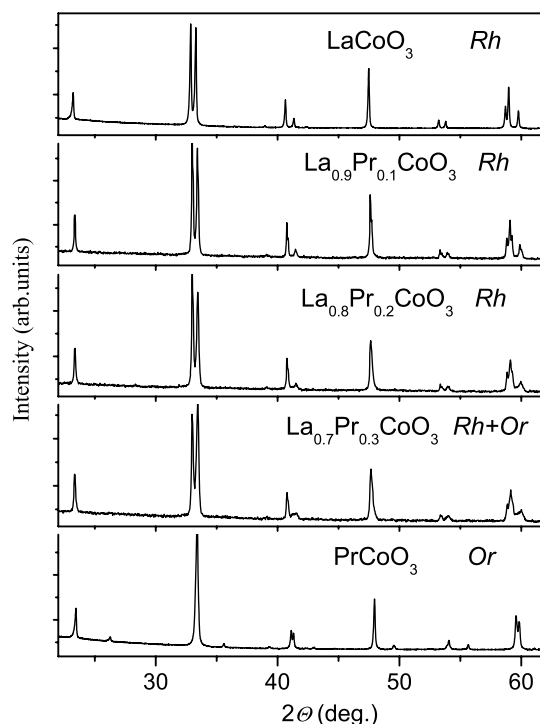


Figure 1. XRD patterns of $\text{La}_{1-x}\text{Pr}_x\text{CoO}_3$ materials (Cu $\text{K}\alpha$ radiation) in comparison with the parent LaCoO_3 and PrCoO_3 compounds with rhombohedral (Rh) and orthorhombic (Or) perovskite structures.

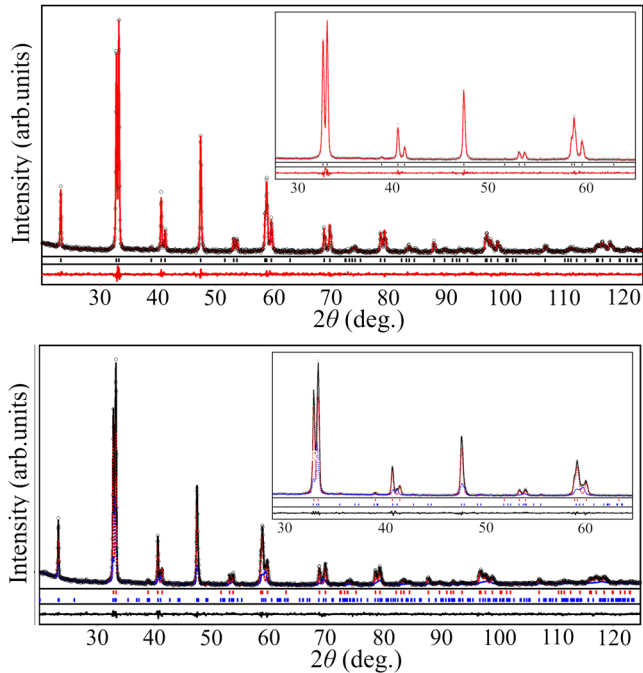


Figure 2. Top panel: graphical results of full-profile Rietveld refinement of $\text{La}_{0.9}\text{Pr}_{0.1}\text{CoO}_3$ structure in the single-phase $R\bar{3}c$ rhombohedral model. Bottom panel: Simultaneous two-phase Rietveld refinement showing the presence of 71 wt% of $R\bar{3}c$ and 29 wt% of $Pbnm$ perovskite phases (blue and red curves, respectively) in the $\text{La}_{0.7}\text{Pr}_{0.3}\text{CoO}_3$ sample. Experimental XRD patterns (black circles) are shown in comparison with the calculated patterns (blue and red lines). The difference between measured and calculated profiles is shown as a curve below the diagrams. Short vertical bars indicate the positions of diffraction maxima in $R\bar{3}c$ (red) and $Pbnm$ (blue) structures.

Table 1. Lattice parameters, positional, and displacement parameters of atoms in $\text{La}_{1-x}\text{Pr}_x\text{CoO}_3$ structures.

Atoms	Parameters	$x = 0$	$x = 0.1$	$x = 0.2$	$x = 0.3$	
		$R\bar{3}c$	$R\bar{3}c$	$R\bar{3}c$	$R\bar{3}c$ (71 wt.%)	$Pbnm$ (29 wt.%)
	a , Å	5.4419(2)	5.4393(3)	5.4359(4)	5.4341(3)	5.4407(9)
	b , Å	–	–	–	–	5.3565(8)
	c , Å	13.0885(5)	13.0797(9)	13.069(1)	13.0504(9)	7.594(1)
La/Pr,	x	0	0	0	0	–0.0152(13)
6a in $R\bar{3}c$	y	0	0	0	0	0.0289(9)
c in $Pbnm$	z	1/4	1/4	1/4	1/4	1/4
	B_{iso} , Å ²	0.76(9)	0.79(6)	0.62(5)	0.56(5)	0.60(12)
Co,	x	0	0	0	0	0
6b in $R\bar{3}c$	y	0	0	0	0	1/2
b in $Pbnm$	z	0	0	0	0	0
	B_{iso} , Å ²	0.9(2)	0.79(12)	0.89(10)	1.13(11)	0.9(3)
O1,	x	0.553(5)	0.546(3)	0.546(3)	0.551(3)	0.032(12)
e in $R\bar{3}c$	y	0	0	0	0	0.505(8)
c in $Pbnm$	z	1/4	1/4	1/4	1/4	1/4
	B_{iso} , Å ²	1.6(6)	1.2(4)	0.9(3)	0.7(3)	1.0(18)
O2,	x	–	–	–	–	–0.308(5)
d in $Pbnm$	y	–	–	–	–	0.258(12)
	z	–	–	–	–	0.041(5)
	B_{iso} , Å ²	–	–	–	–	1.0(11)
	R_l	0.038	0.039	0.033	0.043	0.093
	R_p	0.094	0.120	0.122	0.151	0.151

Quantum Design SQUID magnetometer. Similar measurements were also carried out for $\text{La}_{1-x}\text{Pr}_x\text{AlO}_3$ compounds, which were prepared by a combination of solid-state synthesis at 1373 K following by arc-melting in Ar atmosphere.^[31] Comparing data for both systems made it possible to derive properly the contribution of cobalt ions to magnetic susceptibility of $\text{La}_{1-x}\text{Pr}_x\text{CoO}_3$. The obtained experimental data for $\text{La}_{1-x}\text{Pr}_x\text{CoO}_3$ and $\text{La}_{1-x}\text{Pr}_x\text{AlO}_3$ are shown in **Figure 3** and **4**, respectively, and in general, are in agreement with the relevant data in the study by Kobayashi et al.^[23]

The appreciable Curie-like rise of the susceptibility of $\text{La}_{1-x}\text{Pr}_x\text{CoO}_3$ was observed at low temperatures which obeys a relation

$$\chi(T) \simeq C_{\text{imp}}/T + \chi_0 \quad (1) \quad \text{Q6}$$

where C_{imp}/T term is assumed to originate from a small amount of the paramagnetic impurities and χ_0 is the host susceptibility. The corresponding values of parameters in Equation (1), estimated from $\chi(T)$ versus $1/T$ dependence, are shown in **Table 2**. The estimates of Pr ions magnetism at $T \rightarrow 0$ K are also shown in **Table 2**. This magnetism of the Pr ions mainly contributes to χ_0 value of $\text{La}_{1-x}\text{Pr}_x\text{CoO}_3$ compounds with increasing Pr content.

For LaCoO_3 , our value of $\chi_0 \simeq 1.0 \times 10^{-3}$ emu mol⁻¹ (herein after referred to as $\chi_0(\text{LaCoO}_3)$) coincides in order of magnitude

1 fit between calculated and experimental profiles was achieved in
2 the space group $R\bar{3}c$ (**Figure 2**, top panel).

3 In contrast, only including the additional $Pbnm$ phase into the
4 full profile Rietveld refinement procedure well-described all the
5 diffraction features of the $\text{La}_{0.7}\text{Pr}_{0.3}\text{CoO}_3$ material, which cannot
6 be satisfactorily fitted in the single-phase perovskite model
7 (**Figure 2**, bottom panel). Refined structural parameters of the
8 materials studied are shown in **Table 1**. In the refinement
9 procedure, the unit cell dimensions, atomic coordinates, and
10 displacement parameters of atoms were refined together with
11 profile parameters and corrections for the adsorption and instru-
12 mental sample shift.

13 The obtained structural parameters of $\text{La}_{1-x}\text{Pr}_x\text{CoO}_3$ perov-
14 skite materials studied in this work agreed well with the
15 structural data for the parent LaCoO_3 and PrCoO_3 compounds
16 and the mixed lanthanum–praseodymium cobaltites,^[29,30]
17 proving the existence of two kinds of solid solutions in
18 LaCoO_3 – PrCoO_3 pseudobinary system.

19 2.2. Magnetic Properties

20 For the synthesized samples of $\text{La}_{1-x}\text{Pr}_x\text{CoO}_3$, the temperature
21 dependence of their magnetic susceptibility was measured in the
22 range from 5 to 400 K in a magnetic field of 1 T, using a

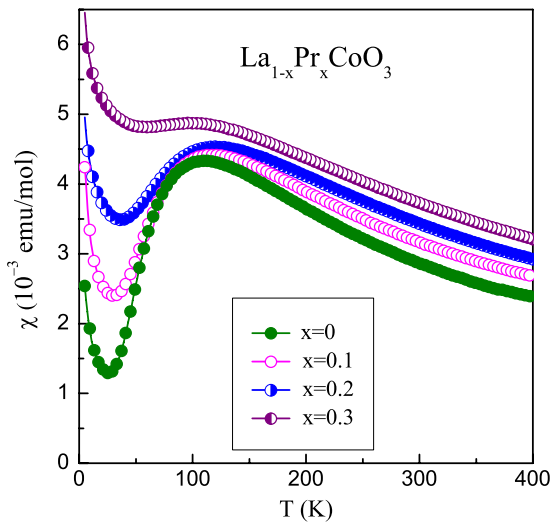


Figure 3. Temperature dependencies of magnetic susceptibility of $\text{La}_{1-x}\text{Pr}_x\text{CoO}_3$ compounds.

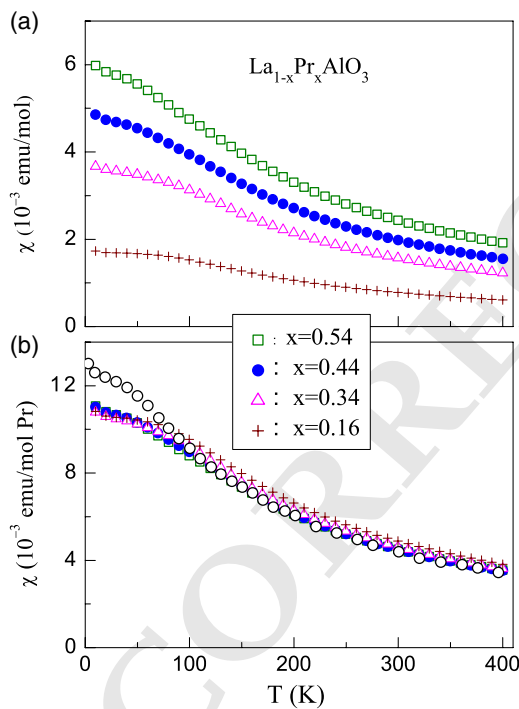


Figure 4. a) Temperature dependencies of the molar magnetic susceptibility of $\text{La}_{1-x}\text{Pr}_x\text{AlO}_3$ compounds and b) their values normalized per mole of Pr. (e)—data for $x=1$ from the study by Kobayashi et al.^[23] (some deviation from the general regularity below 100 K is apparently due to manifestation of the structural phase transition in PrAlO_3).^[31]

Table 2. Estimated from Equation (1), the Curie constant of the paramagnetic impurities C_{imp} (in units of $10^{-3} \text{ K emu mol}^{-1}$) and host susceptibility χ_0 in the low-temperatures region for $\text{La}_{1-x}\text{Pr}_x\text{CoO}_3$ compounds together with contribution of the Pr ions χ_{Pr} at $T \rightarrow 0 \text{ K}$ (both in units of $10^{-3} \text{ emu mol}^{-1}$). For details of the χ_{Pr} estimates, see Section 4.

x	C_{imp}	χ_0	$\chi_{\text{Pr}}(T \rightarrow 0 \text{ K})$
0.0	8.4	1.0	–
0.1	11.4	2.1	1.06
0.2	8.6	3.4	2.12
0.3	8.5	4.85	3.18

LaCoO_3 .^[33–37] For all our samples of $\text{La}_{1-x}\text{Pr}_x\text{CoO}_3$, the presence of these foreign phases was apparently confirmed by a sharp divergence of the $\chi(T)$ dependencies at $T \approx 85 \text{ K}$ measured in $H = 0.01 \text{ T}$ with cooling in a field (FC) and with heating in a field after cooling in zero field (ZFC). This typical low field manifestation of the foreign magnetic phases in cobaltites^[33–37] was not detected in our FC and ZFC data for $H = 1 \text{ T}$.

In comparison with $\text{La}_{1-x}\text{Pr}_x\text{CoO}_3$, in $\text{La}_{1-x}\text{Pr}_x\text{AlO}_3$ compounds, the impurity Curie-like effect was noticeably smaller and it can be omitted in the subsequent discussion. In addition, as shown in Figure 4b, the values of χ per mole of Pr for $\text{La}_{1-x}\text{Pr}_x\text{AlO}_3$, estimated from data for different concentrations of Pr, coincide well with each other, that indicates an approximate additivity of the Pr contribution in this system. This additivity also simplified the account of the Pr magnetism when extracting the temperature-induced spin contribution of the Co^{3+} ions from the total susceptibility of $\text{La}_{1-x}\text{Pr}_x\text{CoO}_3$.

The uniform pressure effect on the magnetic susceptibility of $\text{La}_{1-x}\text{Pr}_x\text{CoO}_3$ was studied under helium gas pressure P up to 2 kbar, using a pendulum-type magnetometer.^[38] To eliminate the effect on susceptibility of the temperature changes when pressure was applied, the measurements were carried out at fixed temperatures 78, 150, and 300 K. The relative experimental errors did not exceed 0.1% for the used magnetic field $H = 1.7 \text{ T}$.

The experimental dependencies of $\chi(P)$ for the studied $\text{La}_{1-x}\text{Pr}_x\text{CoO}_3$ compounds are shown in Figure 5, 6, and 7, being close to linear within the experimental errors and the used interval of pressures. As shown from Figure 5, a huge decrease in the susceptibility with increasing pressure was found at $T = 78 \text{ K}$, which amounts to about 10% per kbar for LaCoO_3 . With increasing temperature, the pressure effect value decreased markedly, and it was an order of magnitude smaller at room temperature. For different temperatures, the obtained pressure derivatives of magnetic susceptibility, $d \ln \chi / dP \equiv (\Delta \chi / \chi) / \Delta P$ at $P \rightarrow 0$, for the studied compounds are shown in Table 3 together with the values of χ at $P = 0$.

3. Details and Results of Electronic Structure Calculations for PrCoO_3

To shed light on the magnetic properties of $\text{La}_{1-x}\text{Pr}_x\text{CoO}_3$ system, we have carried out the calculations of electronic structure for LaCoO_3 and PrCoO_3 compounds. The details of

1 with the corresponding literature data, e.g., 0.65,^[13] 0.50,^[32] and
2 0.16,^[14] in units of $10^{-3} \text{ emu mol}^{-1}$. We assume that noticeable
3 difference in the reported values of χ_0 may be due to manifesta-
4 tion of a small and different amount of the magnetically ordered
5 clusters, which were usually observed in the real crystals of

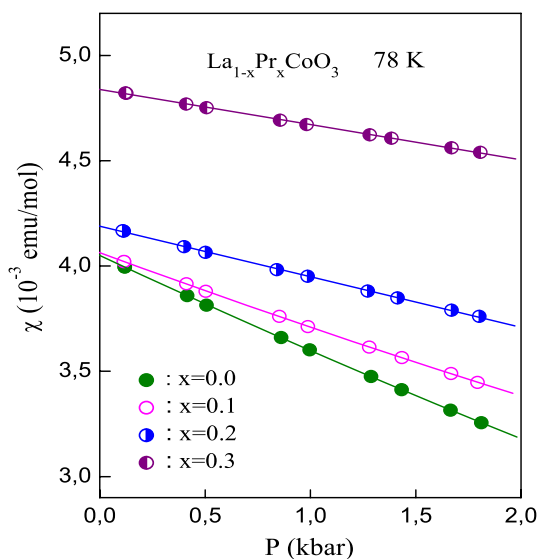


Figure 5. Pressure dependence of magnetic susceptibility for $\text{La}_{1-x}\text{Pr}_x\text{CoO}_3$ compounds at temperature 78 K (the magnitude of the error is less than the size of the symbols).

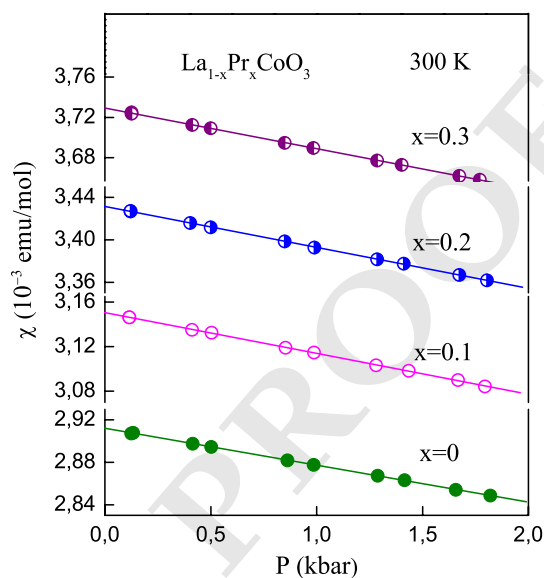


Figure 7. Pressure dependence of magnetic susceptibility for $\text{La}_{1-x}\text{Pr}_x\text{CoO}_3$ compounds at temperature 300 K (the magnitude of the error is less than the size of the symbols).

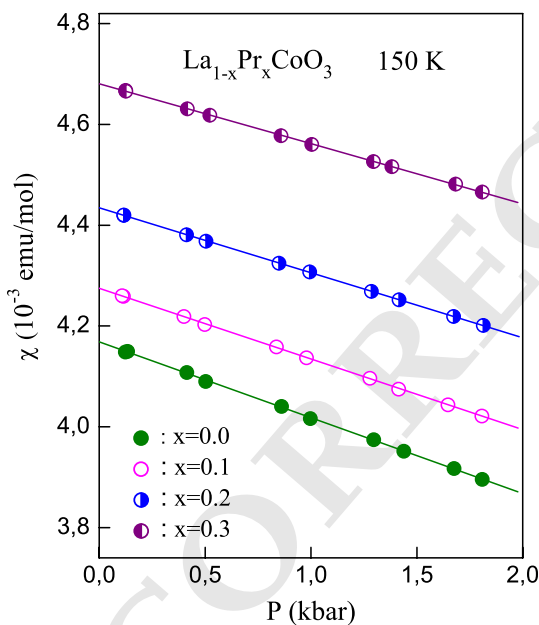


Figure 6. Pressure dependence of magnetic susceptibility for $\text{La}_{1-x}\text{Pr}_x\text{CoO}_3$ compounds at temperature 150 K (the magnitude of the error is less than the size of the symbols).

Table 3. Magnetic susceptibility χ at $P = 0$ and its pressure derivative $d \ln \chi / dP$ for $\text{La}_{1-x}\text{Pr}_x\text{CoO}_3$ compounds at $T = 78, 150,$ and 300 K.

x	$\chi [10^{-3} \text{emu mol}^{-1}]$			$-d \ln \chi / dP [\text{Mbar}^{-1}]$		
	78 K	150 K	300 K	78 K	150 K	300 K
0.0	4.05	4.17	2.91	115 ± 5	36 ± 1	12.0 ± 0.4
0.1	4.06	4.27	3.15	90 ± 4	33 ± 1	11.6 ± 0.4
0.2	4.19	4.43	3.43	57 ± 3	29 ± 1	11.3 ± 0.4
0.3	4.84	4.68	3.73	35 ± 2	26 ± 1	10.8 ± 0.4

1 corresponding calculations for LaCoO_3 are given in the studies
2 by Panfilov et al.^[20,21] In contrast to rhombohedral LaCoO_3 ,
3 PrCoO_3 is orthorhombic. As was shown in the studies by
4 Pandey et al. and Topsakal et al.,^[39,40] the DFT-LSDA approxima-
5 tion predicts an incorrect metallic ground state of PrCoO_3 .
6 Actually, its ground state is a paramagnetic insulator with the
7 low-spin state of Co^{3+} ion.^[41] There is the singlet ground state
8 of Pr^{3+} ions, and only Van Vleck-type magnetization remains

1 at low temperatures.^[41,42] To obtain the semiconducting
2 ground state of PrCoO_3 , it is necessary to use the DFT+ U
3 formalism.^[39,40]

4 The present calculations of electronic structure for orthorhombic
5 PrCoO_3 were carried out using a linearized augmented plane
6 wave method with full potential (FP-LAPW, Elk implementa-
7 tion).^[43] The results of the FP-LAPW method were compared
8 with the corresponding calculations carried out using the
9 Quantum-Espresso code.^[44,45] We have used the projector-
10 augmented wave (PAW) potentials,^[46,47] which are directly appli-
11 cable for the Quantum Espresso code. The DFT+ U approach was
12 used within the generalized gradient approximation (GGA) for
13 the exchange-correlation functional.^[48] The on-site Coulomb
14 interaction, U , and exchange interaction, J , parameters were
15 adopted according to the study by Pandey et al.^[39] ($U = 3.5$ eV,
16 $J = 1.0$ eV, for Co 3d, and $U = 3.5$ eV, $J = 0.7$ eV, for Pr 4f elec-
17 trons, respectively).

18 Our calculations have provided a dielectric ground state for the
19 LS configuration of PrCoO_3 with the energy gap about 1 eV,
20 which is close to the experimental value.^[39,40] For this LS state
21 of Co^{3+} , the valence band is formed by t_{2g} states of cobalt and
22 2p oxygen orbital, whereas the conduction band is formed by

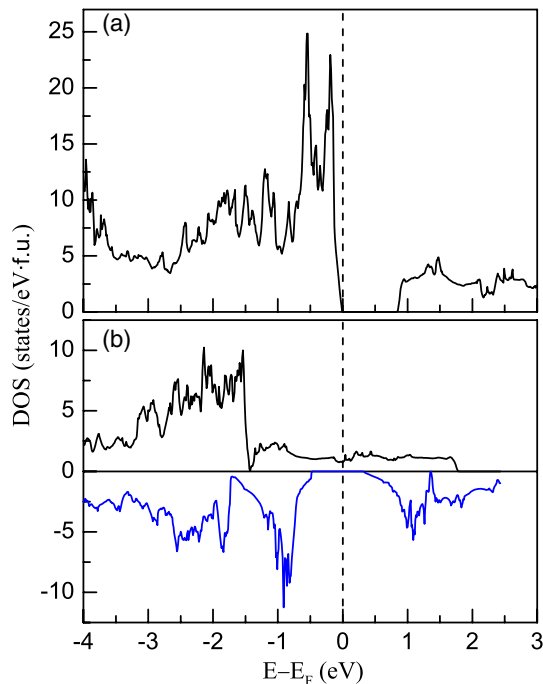


Figure 8. a) Density of electronic states for the LS configuration of cobalt ions in PrCoO₃; b) DOS for the IS configuration for different spin directions. The Fermi level is marked by a dashed vertical line.

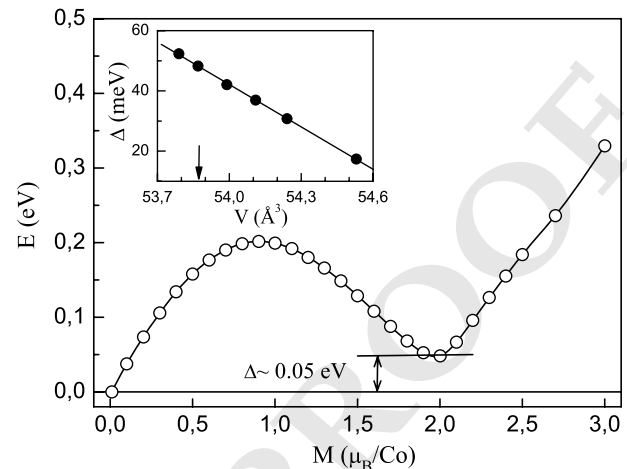


Figure 9. Dependence of the total energy on magnetic moment of Co³⁺ ion for PrCoO₃ calculated by the fixed spin moment method at the theoretical equilibrium volume. The energies are given for the formula unit relative to the ground-state LS ($M = 0$). In the inset: the volume dependence of the energy difference between the IS and LS states, Δ ; the arrow indicates the value of the theoretical equilibrium volume.

1 e_g states of cobalt. The calculated density of electronic states
2 (DOS) for the ground state of PrCoO₃ is shown in **Figure 8a**.
3 The main features of the calculated electronic structure for
4 the LS state of PrCoO₃ appeared to be in agreement with the
5 results of previous calculations.^[39,40]

6 We have also calculated the volume dependence of the total
7 energy $E(V)$ and obtained the value of equilibrium volume $V_{th} \cong$
8 53.9 \AA^3 for the formula unit of orthorhombic PrCoO₃. This the-
9 oretical value of the volume is appeared to be close to the experi-
10 mental value at $T = 12 \text{ K}$ (53.99 \AA^3).^[49]

11 To study the magnetic properties of PrCoO₃ we have used the
12 fixed spin moment (FSM) method.^[27,50] The results of FSM cal-
13 culations for the total energy E of PrCoO₃ are shown in **Figure 9**
14 as a function of magnetic moment of Co³⁺ ion. A pronounced
15 minimum in the $E(M)$ dependence was revealed at $M \cong 2\mu_B$,
16 indicating the presence of the intermediate spin state of Co³⁺
17 ion in PrCoO₃ ($S = 1$). Its energy is slightly higher ($\cong 0.05 \text{ eV}$)
18 than the energy of the ground LS state of Co³⁺ ions ($S = 0$),
19 whereas the HS state ($S = 2$), according to our calculations,
20 has a much higher energy ($\cong 0.6 \text{ eV}$).

21 We have also calculated the volume dependence of the total
22 energy difference between the IS and LS states in PrCoO₃,
23 $\Delta = E_{IS} - E_{LS}$, for isotropic volume changes, which is shown
24 in the inset in **Figure 9** and described by the derivative $d\Delta/d$
25 $\ln V \cong -2.5 \text{ eV}$. It corresponds to a significant increase in Δ
26 under pressure. In contrast, when the lattice of PrCoO₃ is
27 expanding, the IS state approaches LS. Basically, this indicates
28 the possibility of the LS–IS spin states crossover when the vol-
29 ume increases due to thermal expansion. In this connection,
30 it should be noted, that shown in **Figure 9b** spin-polarized

DOS of IS state was calculated with the FSM method for 1
 $T = 0 \text{ K}$. The band structure calculation at high temperatures 2
is extremely complicated problem, not solved satisfactory within 3
the density functional theory. Therefore, one cannot extrapolate 4
this “ferromagnetic” half-metal IS state to the region of high tem- 5
peratures. Actually, the experimental data of Tachibana et al.^[51] 6
definitely indicate, that PrCoO₃ is nonmagnetic insulator up to 7
temperatures of about 600 K. 8

4. Discussion 9

It is commonly assumed that the unusual temperature dependence 10
of $\chi(T)$ in LaCoO₃ is caused by the temperature-induced 11
gradual transition of the Co³⁺ ions from the nonmagnetic LS 12
state ($S = 0$) to a magnetic state with an IS ($S = 1$) and/or to 13
the high spin state HS ($S = 2$). 14

For La_{1-x}Pr_xCoO₃, the $\chi(T)$ dependence, considering para- 15
magnetic impurities, is given by 16

$$\chi(T) = \chi_{Co}(T) + \chi_{0(LaCoO_3)} + C_{imp}/T + \chi_{Pr}(T) \quad (2)$$

Here $\chi_{Co}(T)$ is the temperature-induced contribution of the 17
Co³⁺ ions; $\chi_{0(LaCoO_3)}$, the temperature-independent host suscep- 18
tibility which is presumably determined by the dominant Van 19
Vleck paramagnetism of the Co³⁺ ions,^[13,16] C_{imp} the impurity 20
Curie constant, $\chi_{Pr}(T)$ the contribution of the Pr ions. To study 21
the evolution of the spin state of cobalt ions in La_{1-x}Pr_xCoO₃, it 22
is necessary to extract properly their contribution, χ_{Co} , from the 23
total magnetic susceptibility of the compounds. Some problems 24
arise in this way already in the reference LaCoO₃ compound. 25
According to the literature data, the real crystals of this material 26
contain a certain number of magnetically ordered clusters 27
formed by crystal defects,^[33] nanostructures,^[34,35] surface mag- 28
netism of the Co ions,^[36] or by foreign Co₃O₄ phase,^[37] which 29

1 substantially distort the temperature dependence of the intrinsic
2 magnetic susceptibility in the temperature range below 85 K.
3 This makes it difficult to quantify the low-temperature data
4 and, in particular, probably explains the considerable scatter of
5 literature data for LaCoO₃ on the magnitude of χ_0 . In view of
6 the foregoing, further analysis of the experimental data was
7 carried out for a temperature region above 85 K, where manifesta-
8 tion of the foreign magnetic phases is assumed to be substan-
9 tially suppressed.

10 To extract the contribution of the Co³⁺ ions, χ_{Co} , from the total
11 magnetic susceptibility of La_{1-x}Pr_xCoO₃ compounds with Pr
12 content x , we used the expression

$$\chi_{\text{Co}}(T) = \chi(T) - \chi_0(\text{LaCoO}_3) - C_{\text{imp}}/T - x \cdot \chi_{\text{PrAlO}_3}(T) \quad (3)$$

13 It follows from Equation (2), assuming $\chi_{\text{Pr}}(T) = x \cdot \chi_{\text{PrAlO}_3}(T)$.
14 Here we have accepted that for all compounds the value
15 $\chi_0(\text{LaCoO}_3) \approx 0.2 \times 10^{-3} \text{ emu mol}^{-1}$, which is equal to the theoret-
16 ical estimate of the Van Vleck paramagnetism of the Co³⁺ ions^[52]
17 and fairly close to the observed χ_0 value in the most perfect
18 crystals of LaCoO₃.^[14,20] The individual values of the impurity
19 Curie constant, C_{imp} , were taken from Table 2. To estimate the
20 contribution to $\chi(T)$ of the Pr ions, $x \cdot \chi_{\text{PrAlO}_3}(T)$, we have taken
21 the temperature dependence of molar susceptibility of PrAlO₃,
22 $\chi_{\text{PrAlO}_3}(T)$, averaged over our data in Figure 4b. The latter is char-
23 acterized by the value $\chi_{\text{PrAlO}_3}(0) \approx 10.6 \times 10^{-3} \text{ emu mol}^{-1}$, which
24 was used to estimate the values of low temperature contribution
25 of the Pr ions, $x \cdot \chi_{\text{PrAlO}_3}(0)$, shown in Table 2. For $T \geq 150 \text{ K}$, the
26 $\chi_{\text{PrAlO}_3}(T)$ dependence obeys the Curie-Weiss law with reason-
27 able values of the Curie constant $C \approx 1.7 \text{ K emu mol}^{-1}$ and the
28 paramagnetic Curie temperature $\Theta \approx -75 \text{ K}$.

29 The resulted dependencies of $\chi_{\text{Co}}(T, x)$ are shown in
30 **Figure 10**. They demonstrate that with increasing Pr content,
31 there is a noticeable shift of the $\chi_{\text{Co}}(T)$ maximum to higher tem-
32 peratures with a simultaneous decrease in its height. This effect
33 is very similar to the behavior of the $\chi(T)$ isobars in LaCoO₃ with
34 increasing pressure,^[19] and it can be considered as manifestation

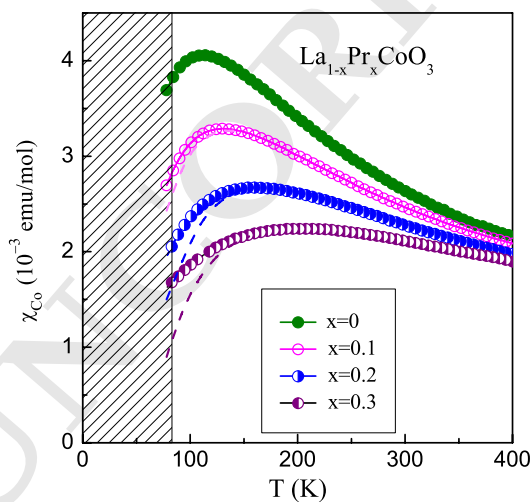


Figure 10. Temperature-induced contribution of the Co³⁺ ions, $\chi_{\text{Co}}(T)$, to magnetic susceptibility of La_{1-x}Pr_xCoO₃ for different Pr content x together with the proposed refinements at low temperatures (dashed lines, see text for details).

of the chemical pressure effects in La_{1-x}Pr_xCoO₃ due to the lat-
tice volume decrease with increase in the Pr content.

As was shown, for example, in the studies by Zobel et al. and Baier et al.^[13,14] for LaCoO₃, at low and moderate temperatures, the $\chi_{\text{Co}}(T)$ term in Equation (2) can be properly described with the LS→IS transition scenario by an expression for the two-level system^[13-15] with the energy difference Δ for these levels

$$\chi_{\text{Co}}(T) = \frac{N_A g^2 \mu_B^2 S(S+1)}{3k_B T} w(T) \equiv \frac{C}{T} w(T) \quad (4)$$

Here, the factor C/T describes the Curie-type susceptibility of the excited state, N_A is the Avogadro number, μ_B the Bohr magneton, k_B the Boltzmann constant, g the Lande factor, and S the spin number. The factor $w(T)$ determines the population of the excited state with temperature

$$w(T) = \frac{\nu(2S+1)e^{-\Delta/T}}{1 + \nu(2S+1)e^{-\Delta/T}} \quad (5)$$

where $2S+1$ and ν are the spin and orbital degeneracies of the excited state, Δ is the difference between the energies of excited and ground states, expressed in units of temperature T . In addition, in the framework of this approach, the parameter Δ also depends on temperature by the relation resulted from Equation (5)^[16]

$$\Delta(T) = T \ln \left[\nu(2S+1) \frac{1 - w(T)}{w(T)} \right] \quad (6)$$

In the following examination of the experimental data within the aforementioned approach, we used the set of model parameters from the studies by Zobel et al., Baier et al., and Knížek et al.^[13,14,16] $g = 2$, $S = 1$, $\nu = 1$ (it is assumed, that the orbital degeneracy of IS state is lifted due to local distortions of the crystal lattice).

Using the experimental dependence $\chi_{\text{Co}}(T, x)$ (Figure 10) and Equation (4) and (6), we have estimated the temperature dependence of the excited-state energy, $\Delta(T)$, in La_{1-x}Pr_xCoO₃ compounds for different Pr content x , which is shown in **Figure 11**. As shown, there is a noticeable decrease in $\Delta(T)$ with increasing temperature. In particular, for $x = 0$, the value of $\Delta \approx 155 \text{ K}$ at $T \approx 80 \text{ K}$ falls down to $\Delta \approx 0$ at $T \approx 250 \text{ K}$, being close in magnitude and temperature dependence to the available literature data for LaCoO₃.^[16] Another feature of the $\Delta(T, x)$ behavior is the strong growth of Δ at fixed temperature with increasing x . According to Figure 11, the rate of Δ change with x is about $\partial\Delta/\partial x \approx 520, 650$, and 770 K at $T \approx 150, 200$, and 300 K , respectively, giving the averaged value $\partial\Delta/\partial x = 650 \pm 120 \text{ K}$. One can presume that this effect to be due to a decrease in the cell volume with increasing Pr concentration x . Therefore, we have estimated the chemical pressure effect on Δ

$$\frac{\partial\Delta}{\partial P} = - \frac{\partial\Delta}{\partial x} \left(B \frac{\partial \ln V}{\partial x} \right)^{-1} = 14 \pm 4 \text{ K kbar}^{-1} \quad (7)$$

using our room temperature experimental data on the volume change with x , $\partial \ln V / \partial x \approx -0.03$, and the bulk modulus value $B \approx 1.5 \text{ Mbar}$.^[53] It should be noted that to specify properly the magnitude of the chemical pressure effect at different

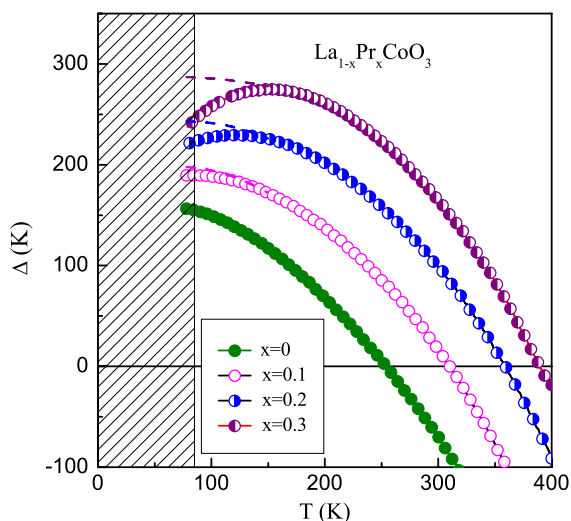


Figure 11. Temperature dependence of the excited state energy Δ in $\text{La}_{1-x}\text{Pr}_x\text{CoO}_3$ compounds for different Pr contents. The dashed lines at low temperatures are corrections for an anticipated manifestation of the foreign magnetic phases (see text for details).

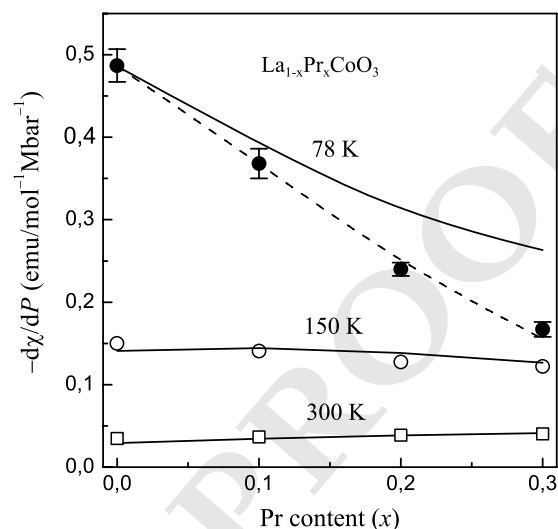


Figure 12. Experimental data on the pressure derivative of magnetic susceptibility, $d\chi/dP$, for $\text{La}_{1-x}\text{Pr}_x\text{CoO}_3$ compounds versus Pr content at different temperatures (points, for $T = 150$ and 300 K, the experimental errors do not exceed the size of the symbols) and their model description by Equation (8) (the solid lines). The dashed line is an improved model description of the data for $T = 78$ K, considering an anticipated manifestation of the foreign magnetic phases in $\chi(T)$ (see text for details).

1 temperatures, it is necessary to consider the temperature
2 dependencies of the bulk modulus $B(T)$ and, especially, the
3 $\partial \ln V(T)/\partial x$ value, originated from difference in the thermal
4 expansion of the compounds due to the peculiarities of manifesta-
5 tion of the spin crossover.^[13,14,54,55]

6 To analyze our experimental data on the hydrostatic pressure
7 effect in magnetic susceptibility, we assumed that its magnitude
8 is predominantly determined by the contribution of $\chi_{\text{Co}}(T)$,
9 i.e., $d\chi(T)/dP \simeq d\chi_{\text{Co}}(T)/dP$. According to Equation (4) and (6),
10 the derivative $d\chi_{\text{Co}}(T)/dP$ can be expressed as follows

$$\frac{d\chi_{\text{Co}}(T)}{dP} = -\frac{\chi_{\text{Co}}(T)}{T} \left[1 - T \frac{\chi_{\text{Co}}(T)}{C} \right] \frac{d\Delta}{dP}. \quad (8)$$

11 Here, the only fitting parameter is the derivative $d\Delta/dP$,
12 whose value is chosen according to the best agreement of the
13 expression (8) with experiment.

14 The obtained for $\text{La}_{1-x}\text{Pr}_x\text{CoO}_3$ experimental values of
15 $d\chi/dP$ ($\equiv \chi d \ln \chi / dP$, see Table 3), are shown in **Figure 12**, as a
16 function of Pr content at $T = 78, 150$, and 300 K. Here, the solid
17 lines correspond to the model description, according to
18 Equation (8), using the values of $\chi_{\text{Co}}(T)$ in Figure 10, the Curie con-
19 stant $C = 1 \text{ Kemu mol}^{-1}$ and the values of $d\Delta/dP = 14, 13$, and
20 16 Kkbar^{-1} at $T = 78, 150$, and 300 K, respectively. As shown,
21 there is a reasonable agreement of the model (8) with the experi-
22 mental data at $T = 150$ and 300 K, whereas at $T = 78$ K, the
23 agreement is somewhat worse. We believe that this is due to
24 using in Equation (8), the overestimated values of χ_{Co} , arising
25 from the manifestation of foreign impurity phases, which
26 probably takes place at lower temperatures. In Figure 10, the
27 proposed dependencies $\chi_{\text{Co}}(T)$ in $\text{La}_{1-x}\text{Pr}_x\text{CoO}_3$ are shown by
28 dashed lines for different x in the range $78 - 150$ K. This correc-
29 tion provides agreement between the model and the experimen-
30 tal data at $T = 78$ K (dashed line in Figure 12), and, in turn,
31 improves the shape of the $\Delta(T)$ dependence (dashed lines in

Figure 11). It should be noted that the aforementioned improve-
ments in the model description of the low temperature experi-
mental data provide convincing evidence in favor of the
proposed refinement of the $\chi_{\text{Co}}(T)$ dependencies in Figure 10.

Let us now discuss the hydrostatic pressure effect on the
excited state energy Δ . As was estimated by fitting the model
parameter $d\Delta/dP$ in Equation (8) to obtain the best agreement
with experimental data, the value of $d\Delta/dP$ falls in the range
of $13\text{--}16 \text{ Kkbar}^{-1}$ at different temperatures, being the lowest
in magnitude at $T = 150$ K. The non-monotonic temperature
dependence of this parameter is presumably related to the fact,
that the physical meaning value is the derivative of Δ with respect
to volume, and not to pressure. Then assuming the parameter
 $d\Delta/d \ln V$ to be a constant for the studied compounds and using
the relation

$$d\Delta/dP = -B^{-1}d\Delta/d \ln V \quad (9)$$

we expect that the dependence of $d\Delta/dP$ on temperature can
arise from a temperature dependence of the bulk modulus,
 $B(T)$. In the absence of direct data on the $B(T)$ behavior for
 $\text{La}_{1-x}\text{Pr}_x\text{CoO}_3$ compounds, it should be noted that essential
temperature dependence of some elastic constants was observed
in LaCoO_3 .^[56,57] This dependence, along with the generally
accepted tendency for B to decrease with increasing temperature,
shows a maximum between 150 and 200 K. Such behavior should
lead to a minimum of $d\Delta/dP$ value in this temperature range,
which is in a qualitative agreement with our experimental data.

Summing up the results of analysis of the pressure effects on
magnetic susceptibility in $\text{La}_{1-x}\text{Pr}_x\text{CoO}_3$ compounds, we have
obtained the temperature averaged value of the pressure deriva-
tive for energy of the excited state to be

$$d\Delta/dP = 14.3 \pm 1.5 \text{ K kbar}^{-1} \quad (10)$$

Substituting this value in Equation (9) and using the room temperature value $B \simeq 1.5 \text{ Mbar}$,^[53] we estimate the volume derivative of Δ equal to

$$d\Delta/d \ln V \simeq -21.5 \times 10^3 \text{ K} \simeq -1.9 \text{ eV} \quad (11)$$

The large and negative volume effect on Δ is also supported by theoretical studies for LaCoO_3 and PrCoO_3 . The detailed calculations of the excited state energy Δ and its volume dependence for LaCoO_3 have given the values $\Delta(0) \simeq 230 \text{ K}$ and $d\Delta/d \ln V \simeq 29 \times 10^3 \text{ K} \simeq -2.5 \text{ eV}$.^[20,21] For PrCoO_3 compound, the present DFT+ U calculations have provided the corresponding values $\Delta(0) \simeq 570 \text{ K}$ and $d\Delta/d \ln V \simeq 29 \times 10^3 \text{ K} \simeq -2.5 \text{ eV}$. Therefore, for boundary compounds LaCoO_3 and PrCoO_3 , the theoretical Δ were found substantially different, and in a qualitative agreement with the behavior of Δ in $\text{La}_{1-x}\text{Pr}_x\text{CoO}_3$ compounds for increasing concentration of Pr (Figure 11). In contrast, the volume derivative of Δ appeared to be almost the same in LaCoO_3 and PrCoO_3 , $d\Delta/d \ln V \simeq -2.5 \text{ eV}$, in a reasonable agreement with the experimental estimations for $\text{La}_{1-x}\text{Pr}_x\text{CoO}_3$ compounds, based on the analysis of pressure effects in magnetic susceptibility (Equation (11)). It should be noted that some difference between the experimental and calculated values of $d\Delta/d \ln V$ may be due to uncertainty in experimental bulk moduli, according to Equation (9).

We believe that the estimated strong volume dependence of the excited state energy Δ determines the main mechanism of its temperature dependence originated from the change in volume via thermal expansion. Namely, for LaCoO_3 , a volume growth of about 1.6%^[54] under heating from 0 to 300 K should result in a decrease in Δ by about 330 K, which is reasonably consistent with the behavior of $\Delta(T)$ in Figure 11.

Note that, some refinement of the analysis results and improvements of the used model should consider few factors, which were not considered here. One of them is a possible manifestation in magnetism of the HS states at higher-temperature region. Further, magnetic interactions between the Co^{3+} moments could play some role in the excited states. In addition, to convert experimentally measured pressure derivatives of susceptibility into volume derivatives, one need data on elastic properties of the systems under consideration and their temperature dependence, which are absent at the moment. Nevertheless, we expect that these possible improvements in the model analysis will not lead to noticeable refinements of the obtained parameters, which, in particular, for LaCoO_3 are

$$\Delta \simeq 155 \text{ K at } T = 78 \text{ K}, d\Delta/dP \simeq 14 \text{ K kbar}^{-1}. \quad (12)$$

These estimates are closely consistent with analogous data obtained in the study by Panfilov et al.^[20] from the magnetovolume effect study in single-crystalline LaCoO_3 .

5. Conclusions

In summary, we have studied the effects of temperature and hydrostatic pressure on magnetic susceptibility of $\text{La}_{1-x}\text{Pr}_x\text{CoO}_3$ compounds ($x = 0, 0.1, 0.2,$ and 0.3), supplemented by the

investigation of their crystal structure. The entire set of the obtained experimental data on temperature and pressure effects in the magnetism of this family of compounds has been consistently described within the LS–IS scenario in terms of changes in the population of the excited IS state of Co^{3+} ions with variations in temperature and lattice volume under hydrostatic and chemical pressure.

One of the main results of this work is a quantitative estimation of the anomalously large volume dependence of the excited state energy Δ , which is presumably a primary source of the temperature dependence of this parameter due to the effect of thermal expansion. The revealed large and negative volume effect on Δ is consistent with the results of ab initio calculations for the boundary compounds, LaCoO_3 and PrCoO_3 , which also supports the LS–IS scenario.

In addition, as shown from Equation (7) and (10), the observed for $\text{La}_{1-x}\text{Pr}_x\text{CoO}_3$ similarity between effects of physical and chemical pressure indicates a strong correlation of the Co^{3+} spin state with the lattice volume.

Acknowledgements

A.K. acknowledges the support of the projects CICECO-Aveiro Institute of Materials (ref. UID/CTM/50011/2013) and POCI-01-0145-FEDER-031875, supported by the COMPETE 2020 Program and National Funds through the FCT/MEC, the Operational Program POCI in its FEDER/FNR component, and the Foundation for Science and Technology, in its State Budget component (OE). L.O.V., V.M.H., G.E.G. and A.S.P. acknowledge the partial support of the Ukrainian Ministry of Education and Sciences under project no. 0118U000264 “DB/Feryt.”

Conflict of Interest

The authors declare no conflict of interest.

Keywords

electronic structure calculations, high-pressure effects, magnetic measurements, RCoO_3 compounds, spin crossovers

Received: February 13, 2020

Revised: June 8, 2020

Published online: 36

- [1] B. Raveau, M. Seikh, *Cobalt Oxides: From Crystal Chemistry to Physics*, Wiley-VCH, Weinheim **2012**, p. 344.
- [2] T. Takami, *Functional Cobalt Oxides: Fundamentals, Properties, and Applications*, Pan Stanford Publishing, Singapore **2014**, p. 176.
- [3] B. Raveau, M. Seikh, in: *Handbook of Magnetic Materials*, Vol. 23, (Ed: K. H. J. Buschow), North Holland, Amsterdam, **2015**, p. 161.
- [4] P. Raccach, J. Goodenough, *Phys. Rev.* **1967**, *155*, 932.
- [5] M. A. Señaris, J. B. Goodenough, *J. Solid State Chem.* **1995**, *116*, 224.
- [6] K. Asai, O. Yokokura, N. Nishimori, H. Chou, J. M. Tranquada, G. Shirane, S. Higuchi, Y. Okajima, K. Kohn, *Phys. Rev. B* **1994**, *50*, 3025.
- [7] M. Itoh, I. Natori, S. Kubota, K. Motoya, *J. Phys. Soc. Jpn.* **1994**, *63*, 1486.
- [8] J. Kuneš, V. Křápek, *Phys. Rev. Lett.* **2011**, *106*, 256401.

- 1 [9] V. Křápek, P. Novák, J. Kuneš, D. Novoselov, Dm. M. Korotin,
2 V. I. Anisimov, *Phys. Rev. B* **2012**, *86*, 195104.
- 3 [10] K. Knížek, Z. Jiráč, J. Hejtmánek, P. Novák, W. Ku, *Phys. Rev. B* **2009**,
4 *79*, 014430.
- 5 [11] M. A. Korotin, S. Yy. Ezhov, I. V. Solov'yev, V. I. Anisimov,
6 D. I. Khomskii, G. A. Sawatzky, *Phys. Rev. B* **1996**, *54*, 5309.
- 7 [12] T. Saitoh, T. Mizokawa, A. Fujimori, M. Abbate, Y. Takeda, M. Takano,
8 *Phys. Rev.* **1997**, *55*, 4257.
- 9 [13] C. Zobel, M. Kriener, D. Bruns, J. Baier, M. Grüninger, T. Lorenz,
10 P. Reutler, A. Revcolevschi, *Phys. Rev. B* **2002**, *66*, R020402.
- 11 [14] J. Baier, S. Jodlauk, M. Kriener, A. Reichl, C. Zobel, H. Kierspel,
12 A. Freimuth, T. Lorenz, *Phys. Rev. B* **2005**, *71*, 014443.
- 13 [15] K. Knížek, P. Novák, Z. Jiráč, *Phys. Rev. B* **2005**, *71*, 054420.
- 14 [16] K. Knížek, Z. Jiráč, J. Hejtmánek, M. Veverka, M. Maryško, G. Maris,
15 T. T. M. Palstra, *Eur. Phys. J. B* **2005**, *47*, 213.
- 16 [17] D. P. Kozlenko, N. O. Golosova, Z. Jiráč, L. S. Dubrovinsky,
17 B. N. Savenko, M. G. Tucker, Y. Le Godec, V. P. Glazkov, *Phys.*
18 *Rev. B* **2007**, *75*, 064422.
- 19 [18] J.-Q. Yan, J.-S. Zhou, J. B. Goodenough, *Phys. Rev. B* **2004**,
20 *69*, 134409.
- 21 [19] K. Asai, O. Yokokura, M. Suzuki, T. Naka, T. Matsumoto,
22 H. Takahashi, N. Mōri, K. Kohn, *J. Phys. Soc. Jpn.* **1997**, *66*, 967.
- 23 [20] A. S. Panfilov, G. E. Grechnev, I. P. Zhuravleva, A. A. Lyogenkaya,
24 V. A. Pashchenko, B. N. Savenko, D. Novoselov, D. Prabhakaran,
25 I. O. Troyanchuk, *Low Temp. Phys.* **2018**, *44*, 328.
- 26 [21] A. S. Panfilov, G. E. Grechnev, A. A. Lyogenkaya, V. A. Pashchenko,
27 I. P. Zhuravleva, L. O. Vasylechko, V. M. Hreb, V. A. Turchenko,
28 D. Novoselov, *Phys. B: Condens. Matter* **2019**, *553*, 80.
- 29 [22] K. Sato, M. I. Bartashevich, T. Goto, Y. Kobayashi, M. Suzuki, K. Asai,
30 A. Matsuo, K. Kindo, *J. Phys. Soc. Jpn.* **2008**, *77*, 024601.
- 31 [23] Y. Kobayashi, T. Mogi, K. Asai, *J. Phys. Soc. Jpn.* **2006**, *75*, 104703.
- 32 [24] M. Itoh, J. Hashimoto, *Phys. C* **2000**, *341–348*, 2141.
- 33 [25] J. R. Sun, R. W. Li, B. G. Shen, *J. Appl. Phys.* **2001**, *89*, 1331.
- 34 [26] C. Y. Chang, B. N. Lin, H. C. Ku, Y. Y. Hsu, *Chinese J. Phys.* **2003**,
35 *41*, 662.
- 36 [27] a) K. Schwarz, P. Mohn, *J. Phys. F: Metal Phys.* **1984**, *14*, L129.
37 b) V. L. Moruzzi, P. M. Marcus, K. Schwarz, P. Mohn, *Phys. Rev. B*
38 **1986**, *34*, 1784.
- 39 [28] L. Akselrud, Yu. Grin, *J. Appl. Crystallogr.* **2014**, *47*, 803.
- 40 [29] L. Vasylechko, O. Myakush, Yu. Prots, A. Senyshyn, *Photon Science*,
41 HASYLAB Annual User Report, **2010**, [http://photon-science.desy.de/](http://photon-science.desy.de/annual_report/files/2010/20101085.pdf)
42 [annual_report/files/2010/20101085.pdf](http://photon-science.desy.de/annual_report/files/2010/20101085.pdf)
- 43 [30] O. Myakush, V. Berezovets, A. Senyshyn, L. Vasylechko, *Chem. Met.*
44 *Alloys* **2010**, *3*, 184.
- [31] T. Basyuk, L. Vasylechko, S. Fadeev, I. I. Syvorotka, D. Trots, R. Niewa, *1*
Radiat. Phys. Chem. **2009**, *78*, S97. *2*
- [32] M. Itoh, M. Sugahara, I. Matori, K. Motoya, *J. Phys. Soc. Jpn.* **1995**, *3*
64, 3967. *4*
- [33] J. Androulakis, N. Katsarakis, J. Giapintzakis, *Phys. Rev. B* **2001**, *64*, *5*
174401. *6*
- [34] S. Zhou, L. He, S. Zhao, Y. Guo, J. Zhao, L. Shi, *J. Phys. Chem. C* **2009**, *7*
113, 13522. *8*
- [35] A. M. Durand, D. P. Belanger, T. J. Hamil, F. Ye, S. Chi, *9*
J. A. Fernandez-Baca, C. H. Booth, Y. Abdollahian, M. Bhat, *10*
J. Phys.: Condens. Matter **2015**, *27*, 176003. *11*
- [36] J.-Q. Yan, J.-S. Zhou, J. B. Goodenough, *Phys. Rev. B* **2004**, *70*, 014402. *12*
- [37] A. M. Durand, T. J. Hamil, D. P. Belanger, S. Chi, F. Ye, *13*
J. A. Fernandez-Baca, Y. Abdollahian, C. H. Booth, *J. Phys.: 14*
Condens. Matter **2015**, *27*, 126001. *15*
- [38] A. S. Panfilov, *Low Temp. Phys.* **2015**, *41*, 1029. *16*
- [39] S. K. Pandey, A. Kumar, S. M. Chaudhari, A. V. Pimpale, *J. Phys.: 17*
Condens. Matter **2006**, *18*, 1313. *18*
- [40] M. Topsakal, C. Leighton, R. M. Wentzcovitch, *J. Appl. Phys.* **2016**, *19*
119, 244310. *20*
- [41] S. Tsubouchi, T. Kyomen, M. Itoh, M. Oguni, *Phys. Rev. B* **2004**, *69*, *21*
144406. *22*
- [42] P. Novák, K. Knížek, M. Maryško, Z. Jiráč, J. Kuneš, *J. Phys.: Condens.* *23*
Matter **2013**, *25*, 446001. *24*
- [43] <http://lk.sourceforge.net/> *25*
- [44] P. Giannozzi, et al., *J. Phys. Condens. Matter* **2009**, *21*, 395502. *26* Q7
- [45] <http://www.quantum-espresso.org/> *27* Q8
- [46] A. Dal Corso, *Comput. Mater. Sci.* **2014**, *95*, 337. *28*
- [47] M. Topsakal, R. M. Wentzcovitch, *Comput. Mater. Sci.* **2014**, *95*, 263. *29*
- [48] J. P. Perdew, K. Burke, M. Ernzerhof, *Phys. Rev. Lett.* **1996**, *77*, 3865. *30*
- [49] J. Yu, D. Phelan, D. Louca, *Phys. Rev. B* **2011**, *84*, 132410. *31*
- [50] M. Sieberer, S. Khmelevskyi, P. Mohn, *Phys. Rev. B* **2006**, *74*, 014416. *32*
- [51] M. Tachibana, T. Yoshida, H. Kawaji, T. Atake, E. Takayama-Muromachi, *33*
Phys. Rev. B **2008**, *77*, 094402. *34*
- [52] J. S. Griffith, L. E. Orgel, *Trans. Faraday Soc.* **1957**, *53*, 601. *35*
- [53] T. Vogt, J. A. Hriljac, N. C. Hyatt, P. Woodward, *Phys. Rev. B* **2003**, *36*
67, R140401. *37*
- [54] P. G. Radaelli, S.-W. Cheong, *Phys. Rev. B* **2002**, *66*, 094408. *38*
- [55] K. Berggold, M. Kriener, P. Becker, M. Benomar, M. Reuther, *39*
C. Zobel, T. Lorenz, *Phys. Rev. B* **2008**, *78*, 134402. *40*
- [56] S. Murata, S. Isida, M. Suzuki, Y. Kobayashi, K. Asai, K. Kohn, *Phys. B* *41*
1999, *263–264*, 647. *42*
- [57] T. S. Naing, T. Kobayashi, Y. Kobayashi, M. Suzuki, K. Asai, *J. Phys.* *43*
Soc. Jpn. **2006**, *75*, 084601. *44*

Please complete this form and return it via E-Mail or Fax
 to the Editorial Office at
 Fax.: +49 (0) 6201 – 606 525
 E-mail: pssb@wiley-vch.de

Reprint Order Form

Wiley-VCH Verlag GmbH & Co. KGaA
 Physica Status Solidi B
 Rotherstr. 21
 10245 Berlin
 Germany

Manuscript No.: _____
 Customer No.: (if available) _____
 Purchase Order No.: _____
 Author: _____
 Date: _____

Charges for Reprints in Euro (excl. VAT), prices are subject to change. Minimum order 50 copies; single issues for authors at a reduced price.

No. of pages	50 copies	100 copies	150 copies	200 copies	300 copies	500 copies
1–4	345,—	395,—	425,—	445,—	548,—	752,—
5–8	490,—	573,—	608,—	636,—	784,—	1077,—
9–12	640,—	739,—	786,—	824,—	1016,—	1396,—
13–16	780,—	900,—	958,—	1004,—	1237,—	1701,—
17–20	930,—	1070,—	1138,—	1196,—	1489,—	2022,—
every additional 4 pages	147,—	169,—	175,—	188,—	231,—	315,—

Information regarding VAT: Please note that from German sales tax point of view, the charge for Reprints, Issues or Posters is considered as “supply of goods” and therefore, in general, such delivery is a subject to German sales tax. However, this regulation has no impact on customers located outside of the European Union. Deliveries to customers outside the Community are automatically tax-exempt. Deliveries within the Community to institutional customers outside of Germany are exempted from the German tax (VAT) only if the customer provides the supplier with his/her VAT number. The VAT number (value added tax identification number) is a tax registration number used in the countries of the European Union to identify corporate entities doing business there. Starting with a country code (e.g. FR for France), followed by numbers.

Please send me and bill me for

- no. of reprints airmail (+ 25 Euro)
 surface mail
 Fedex No.: _____
 high-resolution PDF file (330 Euro)
 E-mail address: _____
 Special Offer: _____

If you order 200 or more reprints you will get a PDF file for half price.

Please note: It is not permitted to present the PDF file on the internet or on company homepages.

Cover Posters (prices excl. VAT)

Posters of published covers are available in two sizes:

DIN A2 42 x 60 cm / 17 x 24in (one copy: 39 Euro)

DIN A1 60 x 84 cm / 24 x 33in (one copy: 49 Euro)

Postage for shipping posters overseas by airmail:
+ 25 Euro

Postage for shipping posters within Europe by surface
mail: + 15 Euro

Date, Signature

VAT number: _____

Mail reprints / copies of the issue to:

Send bill to:

I will pay by bank transfer

I will pay by credit card

VISA, Mastercard and AMERICAN EXPRESS

For your security please use this link (Credit Card Token Generator) to create a secure code Credit Card Token and include this number in the form instead of the credit card data. Click here:

https://www.wiley-vch.de/editorial_production/index.php

CREDIT CARD TOKEN NUMBER

						v													
--	--	--	--	--	--	---	--	--	--	--	--	--	--	--	--	--	--	--	--